Electron-tunneling dynamics through a double-barrier structure in the presence of phonons

Jihad M. Mohaidat and Kai Shum
Electrical Engineering Department, Institute for Ultrafast Spectroscopy and Lasers, The City College and The Graduate School of the City University of New York, New York, New York 10031

R. R. Alfano
Electrical Engineering Department and Physics Department, Institute for Ultrafast Spectroscopy and Lasers, The City College and The Graduate School of the City University of New York, New York, New York 10031
(Received 22 February 1993)

Electron-tunneling dynamics through a semiconductor double-barrier structure in the presence of plane-wave phonons is investigated by directly solving the time-dependent Schrödinger equation. The temporal profile of tunneling current density due to an electron wave packet incident at the resonant energy channel E_r is calculated at different lattice temperatures. The magnitude of the tunneling current density is shown to decrease in the presence of the electron-phonon interaction, which is attributed to an increase in the reflected current. The calculated tunneling peak current density is shown to decrease with temperature and is compared with available experimental data.

Since the seminal work of Tsu and Esaki,[1] electron tunneling in semiconductor nanostructures has been of interest for various electronic applications. The double-barrier resonant tunneling device has received special attention because of its electronic-transport properties in high-speed electronics. One of the important issues in the study of electron tunneling in nanostructures is the inelastic scattering through the electron-phonon interaction. Experimentally, Goldman, Tsui, and Cunningham[2] provided evidence that the longitudinal-optical (LO) phonon assists in tunneling in the valley current region of a double-barrier structure. The effect of electron-phonon interaction on tunneling has been theoretically treated in the steady state by several investigators.[3–5] Gelfand, Schmitt-Rink, and Levi[3] obtained the electron tunneling through a thin potential barrier with local Einstein phonons by means of a continued fraction expansion and demonstrated the feedback mechanism by which inelastic scattering alters the probability of elastic scattering. Wingreen, Jacobson, and Wilkins[4] converted the problem to that of scattering of electrons in a single resonant state with phonons and confirmed the experimental results provided by Goldman, Tsui, and Cunningham.[2] Recently a simple independent boson model approach was proposed by Cai *et al.*[5] to calculate the one-dimensional (1D) electron tunneling probability with electron-phonon interaction. They showed how the boundary conditions uniquely determine the transmitted and reflected plane waves. The *dynamics* of electron tunneling through double-barrier structures without phonons has also been treated by several investigators. Collins, Lowe, and Barker[6] showed that the temporal behavior of resonant tunneling is characterized by a time constant of $\tau=2h/\Gamma$, where Γ is the resonant energy width. Guo *et al.*[7] estimated the charge buildup time by calculating the probability of finding the electron inside the quantum well of a double-barrier structure. The tunneling dynamics in the presence of phonons has not been properly treated. Some researchers[8,9] tried to carry out an analogy to electron tunneling with phonons by considering a time-modulated barrier height, where transmitted current was found to have energy sidebands (analogous to absorption or emission of phonon quanta). This analogy is not complete because phonon population and different phonon modes cannot be accounted for.

In this paper, a method was developed to investigate the temporal dynamics of electron tunneling by directly solving the time-dependent Schrödinger equation. This method allows us to calculate several important time constants such as transit time and charge buildup time in the presence of different phonon modes in a semiconductor nanostructure. The method was demonstrated by studying electron-tunneling dynamics though a $GaAs/Al_xGa_{1-x}As$ based double-barrier structure in the presence of plane-wave phonons. The temporal profiles of the tunneling current density are calculated at different temperatures. The magnitude of the current density is shown to decrease when the effect of the electron-phonon coupling on resonant tunneling is taken into account due to inelastic-scattering-induced reflection increase. The temperature dependence of the tunneling peak current density is compared with available experimental data.

The Hamiltonian of the electron and phonon system is given by

$$H=H_e+H_p+H_{e\text{-ph}} . \tag{1}$$

Here H_e is the Hamiltonian for a pure electronic system and can be expressed as

$$H_e=-\frac{\hbar^2}{2}\frac{\partial}{\partial z}\frac{1}{m^*(x)}\frac{\partial}{\partial z}+V_0(z) , \tag{2}$$

where $V_0(z)$ is the potential profile of the selected double-barrier structure. In this work the structure consists of a 45-Å GaAs quantum well sandwiched by two 28-Å $Al_{0.3}Ga_{0.7}As$ barriers.

The $m^*(z)$ is the position-dependent electron effective mass with $0.067m_0$ ($0.092m_0$) taken for GaAs

 ©1993 The American Physical Society

($Al_{0.3}Ga_{0.7}As$), where m_0 is the free-electron mass. H_p is the Hamiltonian for a pure phonon system. In this model the phonon system is considered to be in a dynamic equilibrium state with a characteristic temperature T. Furthermore, the effect of electron-phonon interaction on the phonon system is assumed to be weak enough. Therefore, H_p is neglected in our model. $H_{e\text{-ph}}$ is the Hamiltonian for the electron-phonon interaction and can be expressed as

$$H_{e\text{-ph}}=\left[\sum_{\mathbf{q}} M(\mathbf{q})e^{-i(\mathbf{q}\cdot\mathbf{R}+\omega t)}a_{\mathbf{q}}+\text{H.c.}\right], \tag{3}$$

where $a_{\mathbf{q}}$ and $a_{\mathbf{q}}^{\dagger}$ are the phonon annihilation and creation operators, respectively, $\mathbf{M}(\mathbf{q})$ is the phonon wave-number $\mathbf{q}$-dependent electron-phonon scattering matrix, and $\mathbf{R}(\mathbf{r},z)$ is the electron position. In the following we use a model that replaces $e^{i\mathbf{q}\cdot\mathbf{R}}$ by 1 in the $H_{e\text{-ph}}$ since electrons couple more strongly with long-wavelength phonons ($\mathbf{q}\approx\mathbf{0}$).

Using the above described model, the 1D time-dependent Schrödinger equation for a tunneling electron in a double-barrier structure is simplified and given by

$$ih\frac{\partial\psi}{\partial t}=H_e\psi+(Ve^{-i\omega t}+V^{\dagger}e^{i\omega t})\psi\ , \tag{4}$$

where ψ is the product of the electron and phonon wave functions. V and $V^{\dagger}$ are defined as $V=\Sigma M(q)a_q$, $V^{\dagger}=\Sigma M^{*}(q)a_q^{\dagger}$.

It is difficult to find the wave function directly from Eq. (4) since V and $V^{\dagger}$ contain the phonon wave-vector-dependent electron-phonon scattering matrix and number *operators* of $a_{\mathbf{q}}$ and $a_{\mathbf{q}}^{\dagger}$. However, when we limit the electron-phonon interaction process such that (i) only electrons at the incident energy E can virtually emit (absorb) and then absorb (emit) phonons without net generation or absorption of phonons, and (ii) electrons can only be scattered to the $E\pm\hbar\omega$ states by real emission and absorption processes, then the wave function of the electron-phonon system at the incident energy E in the double-barrier structure can be expressed as

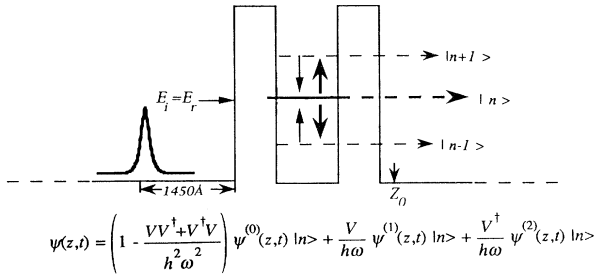

FIG. 1. Tunneling current components in a double-barrier structure with electron-phonon interaction. The double-barrier structure consists of a 45-Å quantum well and two 28-Å barriers with a potential height of 0.28 eV.

$$\psi(z,t)=\left[1-\frac{VV^{\dagger}+V^{\dagger}V}{\hbar^2\omega^2}\right]\psi^{(0)}(z,t)|n\rangle+\frac{V}{\hbar\omega}\psi^{(1)}(z,t)|n\rangle+\frac{V^{\dagger}}{h\omega}\psi^{(2)}(z,t)|n\rangle\ , \tag{5}$$

where $|n\rangle$ is the phonon wave function describing a *single* phonon state. The $\psi^{(0)}(z,t)$, $\psi^{(1)}(z,t)$, and $\psi^{(2)}(z,t)$ are the electronic wave-function components associated with the *single* eigenphonon states $|n\rangle$, $|n-1\rangle$, and $|n+1\rangle$, respectively.

The tunneling process of an electron wave packet with the electron-phonon interaction when the incident energy E is equal to the resonant energy E_r is illustrated using arrows in Fig. 1.

Substituting the wave function given in Eq. (5) into Eq. (4) and multiplying from the left by the phonon state $\langle n|$ and then averaging over the *phonon assembly,* the first component associated with $\psi^{(0)}(z,t)$ in Eq. (6) is obtained. Similarly, multiplying by the phonon states $\langle n-1|$, $\langle n+1|$ will result in the second and the third component associated with $\psi^{(1)}(z,t)$ and $\psi^{(2)}(z,t)$ in Eq. (6), respectively:

$$i\hbar\frac{\partial}{\partial t}\begin{bmatrix}\psi^{(0)}(z,t)\\ \psi^{(1)}(z,t)\\ \psi^{(2)}(z,t)\end{bmatrix}=\begin{bmatrix}H_e & \frac{\hbar\omega g n_q}{1-\zeta}e^{i\omega t} & \frac{\hbar\omega\zeta}{1-\zeta}e^{i\omega t}\\ \hbar\omega(1-\zeta)e^{-i\omega t} & H_e & 0\\ \hbar\omega(1-\zeta)e^{i\omega t} & 0 & H_e\end{bmatrix}\begin{bmatrix}\psi^{(0)}(z,t)\\ \psi^{(1)}(z,t)\\ \psi^{(2)}(z,t)\end{bmatrix}, \tag{6}$$

where $\zeta=g(2n_q+1)$ and g is the electron-phonon coupling constant. In Eq. (6), the average values of $VV^{\dagger}$ and $V^{\dagger}V$ over the phonon assembly were used and are given by

$$\langle VV^{\dagger}\rangle=\sum_q|M(q)|^2(n_q+1)\ ,\quad \langle V^{\dagger}V\rangle=\sum_q|M(q)|^2n_q\ ,\quad \text{and}\quad g=\sum_q[|M(q)|/h\omega]^2\ ,$$

where $n_q=[\exp(\hbar\omega/k_BT)+1]^{-1}$ is the phonon population.

The numerical solution of the time-dependent Schrödinger equation [Eq. (6)] is obtained by first converting it into the following difference equation:[10]

$$\frac{1}{m^*_{j+1}+m^*_j}\begin{bmatrix}\psi^{(0)}_{j+1,l+1}\\ \psi^{(1)}_{j+1,l+1}\\ \psi^{(2)}_{j+1,l+1}\end{bmatrix}+\begin{bmatrix}\eta_j & -\frac{\varepsilon^2}{\hbar}\frac{\omega g n_q}{1-\zeta}e^{-i\omega(l+1)} & -\frac{\varepsilon^2}{\hbar}\frac{\omega\zeta}{1-\zeta}e^{-i\omega(l+1)}\\ -\frac{\varepsilon^2}{\hbar}\omega(1-\zeta)e^{-i\omega(l+1)} & \eta_j & 0\\ \frac{\varepsilon^2}{\hbar}\omega(1-\zeta)e^{i\omega(l+1)} & 0 & \eta_j\end{bmatrix}\begin{bmatrix}\psi^{(1)}_{j,l+1}\\ \psi^{(1)}_{j,l+1}\\ \psi^{(2)}_{j,l+1}\end{bmatrix}$$
$$+\frac{1}{m^*_{j-1}+m^*_j}\begin{bmatrix}\psi^{(0)}_{j-1,l+1}\\ \psi^{(1)}_{j-1,l+1}\\ \psi^{(2)}_{j-1,l+1}\end{bmatrix}+\frac{1}{m^*_{j+1}+m^*_j}\begin{bmatrix}\psi^{(0)}_{j+1,l}\\ \psi^{(1)}_{j+1,l}\\ \psi^{(2)}_{j+1,l}\end{bmatrix}+\frac{1}{m^*_{j-1}+m^*_j}\begin{bmatrix}\psi^{(0)}_{j-1,l}\\ \psi^{(1)}_{j-1,l}\\ \psi^{(2)}_{j-1,l}\end{bmatrix}$$
$$+\begin{bmatrix}-\gamma_j & -\frac{\varepsilon^2\omega g n_q}{\hbar(1-\zeta)}e^{l\omega l} & -\frac{\varepsilon^2\omega\zeta_q}{\hbar(1-\zeta)}e^{-i\omega l}\\ -\frac{\varepsilon^2}{\hbar}\omega(1-\zeta)e^{-i\omega l} & -\gamma_j & 0\\ -\frac{\varepsilon^2}{\hbar}\omega(1-\zeta)e^{i\omega l} & 0 & -\gamma_j\end{bmatrix}\begin{bmatrix}\psi^{(0)}_{j,l}\\ \psi^{(1)}_{j,l}\\ \psi^{(2)}_{j,l}\end{bmatrix}=0\ , \tag{7}$$

where

$$\eta_j=\frac{2\varepsilon^2}{\hbar\delta}i-\frac{\varepsilon^2}{\hbar^2}V_{0j}-\frac{1}{m^*_{j+1}+m^*_j}-\frac{1}{m^*_{j-1}+m^*_j}\quad\text{and}\quad\gamma_j=\frac{2\varepsilon^2}{\hbar\delta}i+\frac{\varepsilon^2}{\hbar^2}V_{0j}+\frac{1}{m^*_{j+1}+m^*_j}+\frac{1}{m^*_{j-1}+m^*_j}\ ,$$

δ (ε) and l (j) are the time (space) interval and index, respectively.

The above three equations for the three components of the electron wave function are coupled with each other through phonon emission and absorption. Each equation represents a complex tridiagonal matrix system. The matrix system is converted into lower and upper diagonal matrices (LU factorization). The forward and backward substitutions along with Gaussian elimination are then used to solve these equations.[11]

In our numerical calculation a spatial mesh size of 0.5 Å, a time mesh size of 1 fs,[12] and a phonon energy of 36.2 meV (GaAs LO-phonon energy) were used. Zero boundary conditions were applied at the two end points 1 μm away from the double-barrier structure.[13]

For our calculation an initial Gaussian wave packet with a central kinetic energy of 90 meV (equal to the resonant energy E_r) and an energy spread of 0.13 meV is placed at the position 1450 Å away from the double-barrier structure in the left lead. The tunneling process is initiated at time $t=0$. This wave packet can simulate a photoexcitation by an ultrafast laser pulse. The development of the electron wave function $\psi(z,t)$ in time is followed as the wave packet moves into and out of the structure.

The 1D current density (J) is calculated at the observation point $\mathbf{z}_0$, 20 Å to the right of the second barrier as indicated in Fig. 1. Substituting the wave function given in Eq. (5) into the quantum-mechanical current-density expression and averaging over the phonon assembly,[5] the total electron current density observed at point $\mathbf{z}_0$ is given by

$$J=\{1-[g(n_q+1)+gn_q]\}^2J_0+gn_qJ_1+g(n_q+1)J_2\ , \tag{8}$$

where

$$J_k=\frac{\hbar}{2m^*i}\left[\psi^{(k)*}\frac{\partial\psi^{(k)}}{\partial z}-\frac{\partial\psi^{(k)*}}{\partial z}\psi^{(k)}\right]\quad k=0,1,2\ .$$

The calculated 1D resonant current-density temporal profiles are shown in Fig. 2 by the solid curve for no phonon coupling, $g=0.0$, the dotted curve for $g=0.1$ and

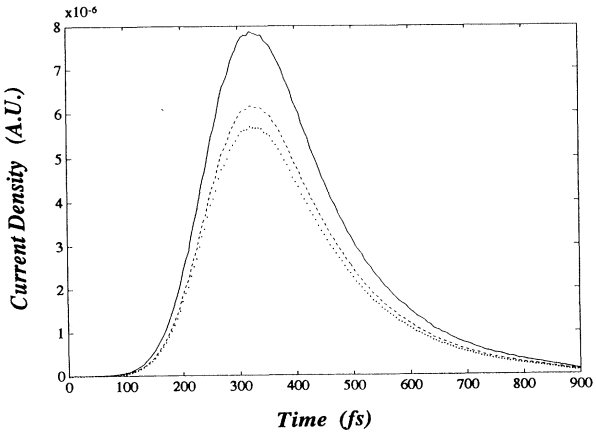

FIG. 2. Temporal behavior of the 1D resonant tunneling current density for the different conditions: (i) the solid curves for coupling constant $g=0.0$, (ii) the dotted curves for $g=0.1$ and $T=300$ K, and (iii) the dashed curves for $g=0.1$ and $T=0$ K.

$T=300$ K, and the dashed curve for $g=0.1$ and $T=0$ K.

Let us discuss these curves, starting with the discussion of the solid curve in Fig. 2 which represents the *elastic* (coherent) resonant tunneling current density at channel E_r. The current reaches a maximum value at 300 fs after the excitation of the electron wave packet at the left lead of the selected structure. This resonant tunneling time is determined by four factors: (i) how far the packet is placed away from the left barrier in the left lead, (ii) the structure dimensions, (iii) how far the observation point is from the right barrier, and (iv) what the central kinetic energy of the packet is. The value of 300 fs implies an average electron traveling speed of 6×10^7 cm/sec which is consistent with the speed calculated using the central kinetic energy of 90 meV indicating coherent tunneling nature. The current density decreases once the wave packet passes the observation point z_0 and decays exponentially with a time constant of 320 fs. The dashed curve in Fig. 2 reflects the *net loss* of tunneling current observed at z_0 due to inelastic scattering at zero temperature. The maximum value of the current density decreases further at 300 K as shown by the dotted curve in Fig. 2 because both real phonon emission and absorption are allowed. It should be noted that the effect on transit time through the double-barrier structure in the presence of phonons is negligible.

In Fig. 3, the calculated temperature dependence of the peak current-density ratio $\{J(T)/J(10\text{ K})\}$ is shown by the solid curve. As can be seen, the peak current density remains almost constant over the temperature range of 0–100 K. However, as the temperature is increased further, the scattering processes increase and the tunneling peak current density starts to decrease. For comparison, the measured data by Bar-Joseph *et al.*[14] are shown by the stars in Fig. 3. The thermionic contribution for the current density predicted by a theory[15] is subtracted from the data point at 300 K. The thermionic contribution for other data points is negligible. It is clear that both calculated and measured peak current density decrease as temperature increases. The difference in the magnitude of measured and calculated data may be due to the fact that our model considers only plane-wave phonons, while in reality the confined, interface, and acoustic phonons should be taken into account.

It should be pointed out that the use of the value

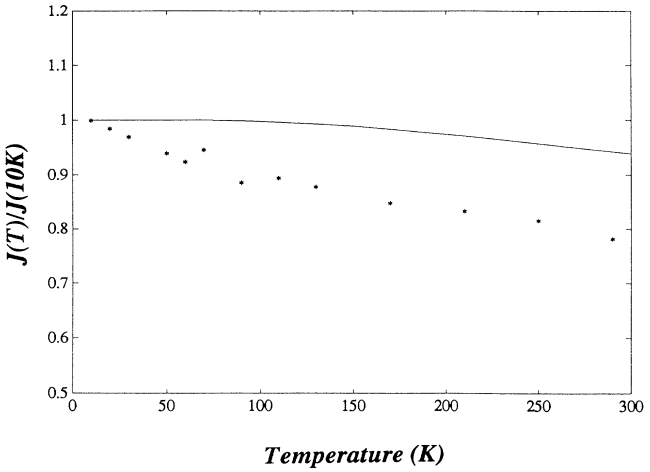

FIG. 3. The temperature dependence of the tunneling current-density peak ratio $J(T)/J(10\text{ K})$. The solid curve is calculated by the model described in the text. The stars indicate the experimental data.

$g=0.1$ is just for demonstrational purposes. The magnitude of phonon-assisted tunneling is smaller for a smaller value of g.[5] The used value for g in our calculations may be slightly overestimated for GaAs/Al_xGa_{1-x}As structures but it may be appropriate for II-VI compound based structures.[4] Finally it should be emphasized that our approach can be used to study the phonon-assisted tunneling dynamics associated with various phonon modes since the realistic electron-phonon scattering matrix as a function of space can be taken care of.

In conclusion, we have demonstrated an approach for studying the dynamics of electron tunneling in the presence of plane-wave phonons in a double-barrier structure. The temporal profiles of a tunneling electron wave packet at different lattice temperatures were presented. It was shown that tunneling current decreases in the presence of electron-phonon interaction. The calculated temperature dependence of the peak current density agrees qualitatively with available experimental data.

This work was supported by the Army Research Office under Grant No. DAAL-89-9-0110. The authors would like to thank Dr. W. Cai for valuable discussions.

[1]R. Tsu and L. Esaki, Appl. Phys. Lett. **22**, 562 (1973).
[2]V. J. Goldman, D. C. Tsui, and J. E. Cunningham, Phys. Rev. B **36**, 7635 (1987).
[3]B. Y. Gelfand, S. Schmitt-Rink, and A. F. J. Levi, Phys. Rev. Lett. **62**, 1683 (1989).
[4]N. S. Wingreen, K. W. Jacobson, and J. W. Wilkins, Phys. Rev. Lett. **61**, 1396 (1988).
[5]W. Cai, T. F. Zheng, P. Hu, B. Yudanin, and M. Lax, Phys. Rev. Lett. **63**, 418 (1989).
[6]S. Collins, D. Lowe, and J. R. Barker, J. Phys. C **20**, 6233 (1987).
[7]H. Gou, K. Diff, G. Neofotistos, and J. Gunton, Appl. Phys. Lett. **53**, 131 (1988).
[8]A. P. Jauho and M. Jonson, Superlatt. Microstruct. **6**, 303 (1989).
[9]A. P. Jauho, Phys. Rev. B **41**, 12 327 (1990).
[10]C. Juang, K. Kuhn, and R. Darling, Phys. Rev. B **41**, 12 047 (1990).
[11]W. Press, B. Flannery, S. Teukolsky, and W. Vetterling, *Numerical Recipes, The Art of Scientific Computing* (Cambridge University Press, Cambridge, 1988), p. 40.
[12]J. M. Mohaidat, K. Shum, and R. R. Alfano, Phys. Rev. B **45**,

3822 (1992).
[13]Under the considered time scale, 1-μm distance away from the barriers is far enough to insure that the packet will not hit the boundary and bounce back to affect the calculations.
[14]I. Bar-Joseph, Y. Gedalyahu, A. Yacoby, T. Woodward, D. Shemla, D. Sivco, and A. Cho, Phys. Rev. B **44**, 8361 (1991).
[15]S. Sze, *Physics of Semiconductors* (Wiley, New York, 1981), p. 256.